JACOB DUELUND KAAS CHRISTENSEN

ATOMIC FORCE MICROSCOPE MEASUREMENTS

OF

NERVES

SUPERVISOR: THOMAS HEIMBURG

Acknowledgements

I would like to thank the Membrane Biophysics Group at Copenhagen University for letting me write this project, especially three people who have been of great help. First I would like to thank my supervisor Thomas Heimburg for the whole idea about the project and taking his time to answer my questions when I did not know what to do. I would also like to thank Andreas Blicher for his help in the laboratory, both in preparing samples aswell as discussion of theory and results. Finally a big thank goes to Rolf J. Pedersen for taking his time to working at the AFM with me, helping me understand the general idea of how it works and showing me how to use it, and taking his time to prepare crayfish nerves for my final experiments.

Abbreviations

AFM: Atomic Force Micropscope

DPPC: Dipalmitoylphosphatidylcholine

DMPC: Dimyristoylphosphatidylcholine

DLPC: Dilauroylphosphatidylcholine

Contents

1 Introduction

Biological membranes are complex structures consisting of a vast number of components, mainly species of lipids and proteins. These membranes are the boundary structures that seperate one environment from another, such as separating the inside of the cell from the external environment, or lesser structures like separation of the cell nucleous from the rest of the cell. The main functions of the membrane are to maintain different concentrations between the two sides of the membrane and be selective to the molecules that enter or exit the cell. The general picture of the membrane is given by the fluid mosaic model by Singer and Nicholson where proteins are able to diffuse in a two dimensional lipid bilayer (Fig. 1.1).
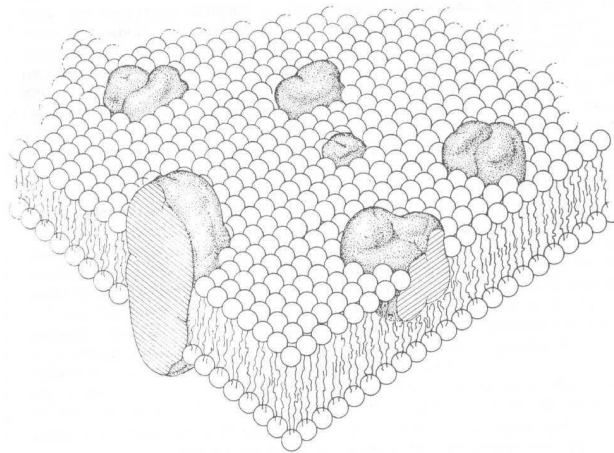

Figure 1.1: Fluid mosaic model. The lipid bilayer is represented by the plane of small balls with two tails each. Proteins are the bigger structures,[2].

This model has been extended since it was proposed, but by looking at this model and the fact that the membrane consists of so many different components in a wide range of compositions, looking at a membrane taken from a living cell indeed is complicated. Therefore model membranes have been made. The first membrane to be investigated was a membrane consisting of the lipid DPPC whereas the other membrane consists of a mixture of DLPC and DMPC. These model membranes will allow more straight forward examination and analysable data than a biological membrane. Though good for prelimenary analyses, model membranes will not be sufficient to describe the nerve of a crayfish, which is the main idea of this project. Generally nerve cells, or neurons, are the constituents of the central nervous system responsible for processing signals from one part of the system to the other, which is basicly the difference between neurons and all other cells. A neuron normally consists of a cell body called the soma, which is connected to the dendrites of the neuron. Dendrites are

1

the structures that recieve neural signals. Transmission of signals along the nerve is done by axons, which are cable like structures than can be very long, up to 2 meters, [5]. In vertebrates (creatures with a spine) neurons, and especially the axons, can be insulated by a membrane called the myelin layer, which improves neural signal transmission, [5]. Because invertebrates do not have these insulating layers around their neurons (at least not to the same degree), their neurons get a lot thicker and are therefore better suited for experiments, which is the reason for using for example a crayfish nerve in experiments.
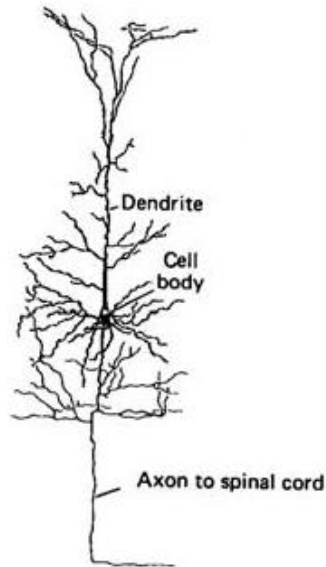
Figure 1.2: Schematic drawing of a pyramidal cell, [5].

An example of a neuron can be seen above. This is the pyramidal cell of the cerebral cortex, a part of the brain. This is a good example of a neuron which shows both the soma, the dendrites and the axon.

This project has mainly been experimental. A big part of the project has been the use of an AFM to image lipids on a mica surface in aqueous solutions and measuring their height profiles to get a solid feeling of the use of the AFM. The reason for choosing single or two lipid mixtures is that it is possible to produce distinct pictures which can be analysed by the theory presented below. The second part of the project has been to image a real biological membrane, namely a nerve taken from the tail of a crayfish. Since a single nerve cannot be cut out, the images will be of a bundle of nerves surrounded by a layer of tissue.

2 Theory

As stated above lipids come in a wide range of species. These can be divided into three groups where the most abundant in biological membranes are phospholipids, which is the class that the lipids in these experiments belong to. Generally phospholipids consists of a polar headgroup and two apolar hydrocarbon chains. This makes phospholipids amphiphilic molecules, meaning that one part (the polar) loves water and that the other part (the apolar) hates water. In Figure 2.1 the lipid DPPC is shown. All bends, where no symbols are shown, represent carbon atoms and the two hydrophobic hydrocarbon chains are the ones to the left, bound to the headgroup by oxygen atoms. From this, one can count that there are 16 carbon atoms in each of the two chains.
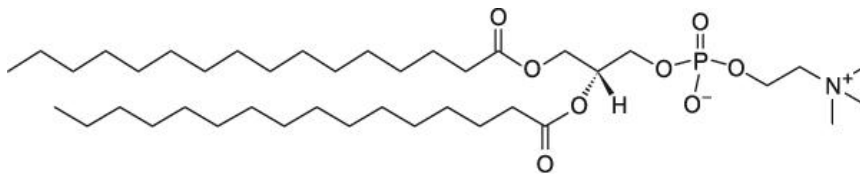

Figure 2.1: Schematic drawing of DPPC, [13].

This number of carbon atoms can vary, changing the physical properties of the lipid, e.g. DLPC has 12 carbon atoms in its chains and DMPC got 14. Further more saturation/unsaturation can be taken into account. This is the fact that there can be double bonds between two carbon atoms, causing the chain to bend. This will also cause different physical properties due to the fact that the space the individual lipid occupies gets bigger when it cannot allign its two hydrocarbon chains parallel to each other.

Because phospholids are amphiphilic they form lipid bilayers, which is the structure that our model membrane consists of. The reason for this is that the lipids want to keep their hydrophobic chains away from the water, and instead let the headgroup phase the water, because this is simply energetically favorable. Therefore the hydrophobic chains are packed inside the membrane whereas polar headgroups on each side faces the water. Bilayers are not the only structures that are formed by lipids interacting. Several phases, like hexagonal phases and sponge phases have been observed. The occurence of different phases is because of different lipids, lipid concentration, ionic strenght etc. Although other phases exists, it is only the bilayer phase that is relevant here.

2.1 Phase transition

It is the hydrocarbon chains that determine the state of the lipid bilayer. To get a deeper understanding of this, one has to look at the bonds between the carbon atoms. The two car-

bon atoms are free to rotate around the bond between them, but there are three certain angles where the energy is at a minimum. The lowest of these three minima is the trans conformation and the two higher energy conformations, with the same energy, are the gauche$^+$ and gauche$^-$ conformations. At sufficiently low temperatures the chains will be ordered in an all-trans configuration, corresponding to the lowest possible energy state. This state is called the gel state. At higher temperatures gauche conformations become more probable resulting in a higher degree of disorder among the chains and at high enough temperatures the chains are fully disordered and the lipids are said to be in the fluid phase. In between these two extremes is the phase transition. This is when the two gauche states and the trans state are found with equal probability, and this transition is related to a specific melting temperature, depending on the lipid species, pressure and so forth.

2.2 Lipid mixtures

Lipids interacting with other species of lipids generally do not yield the same result as lipids interacting with species of their own kind. Having such lipids in a mixture is what you would call a regular solution. On the other hand, if different lipids interact with other lipids almost as they would with their own kind, one can approximate this to a ideal solution where all interactions are the same[1]. For two lipid species with different melting temperatures, interacting as though they are an ideal solution, one can look at a membrane consisting of these, where the lipids can be either in a fluid or a gel state. By introducing the chemical potential μ, one can get a deeper understanding of how the lipid mixture behaves. The chemical potential is the chemical counterpart to gravitational potential or electric potential, meaning that it dictates the movements of particles. Let the chemical potential be defined for each lipid species in either gel or fluid state $\mu_{species}^{state}$. In a thermodynamic equilibrium the chemical potentials of the reagents and products are equal. An example would be the unimolecular reaction where lipid goes from gel to fluid. Let the two lipids be respectively A and B and you obtain

$$\mu_A^{gel} = \mu_A^{fluid} \quad \text{and} \quad \mu_B^{gel} = \mu_B^{fluid} \tag{2.1}$$

Generally the chemical potential of particle i can be written

$$\mu_i = \mu_{i,0} + RT\ln\frac{c_i}{c_0} \tag{2.2}$$

Where the standard chemical potential $\mu_{i,0}$ of particle i is the Gibbs free energy under standard concentration c_0 (1 mol/L), R is the gas constant, T is temperature and c_i is the concentration of particle i. Using $x_{species}^{state}$ as the fraction of a given lipid species, either A or B, in gel or fluid state instead of the fraction of concentrations in (2.2) combined with (2.1), one obtains

$$\frac{x_A^{fluid}}{x_A^{gel}} = \exp\left(-\frac{\mu_{A,0}^{fluid} - \mu_{A,0}^{gel}}{RT}\right) \quad \text{and} \quad \frac{x_B^{fluid}}{x_B^{gel}} = \exp\left(-\frac{\mu_{B,0}^{fluid} - \mu_{B,0}^{gel}}{RT}\right) \tag{2.3}$$

The difference in standard chemical potential between different states is related to the difference in enthalpy ($\Delta H_{i,0}$) and entropy ($\Delta S_{i,0}$) in this way

$$\mu_i = \Delta H_{i,0} - T\Delta S_{i,0} \tag{2.4}$$

---

[1] The 1:10 DLPC : DMPC mixture shows ideal mixture behavior, which can be seen from its heat capacity profile, see Figure **??**

And the relation between entropy difference and melting temperature ($T_{m,i}$) is

$$\Delta S_{i,0} = \frac{\Delta H_{i,0}}{T_{m,i}} \tag{2.5}$$

Putting (2.3), (2.4) and (2.5) together you end up with the following expressions and definitions

$$\frac{x_A^{fluid}}{x_A^{gel}} = \exp\left(-\frac{\Delta H_{A,0}}{R}\left(\frac{1}{T} - \frac{1}{T_{m,A}}\right)\right) \equiv e^{-A} \tag{2.6}$$

And

$$\frac{x_B^{fluid}}{x_B^{gel}} = \exp\left(-\frac{\Delta H_{B,0}}{R}\left(\frac{1}{T} - \frac{1}{T_{m,B}}\right)\right) \equiv e^{-B} \tag{2.7}$$

As x represents the fraction of a lipid species in either gel or fluid state, the sum of the lipid fractions in gel state must be equal to 1, and the same goes for the sum of the lipid fractions in the fluid state, since these sums represent the entire gel and fluid parts of the membrane. Therefore

$$x_A^{gel} + x_B^{gel} = 1 \quad \text{and} \quad x_A^{fluid} + x_B^{fluid} = 1 \tag{2.8}$$

With four equations and four unknowns, one can calculate expressions of x_A^{gel}, x_B^{gel}, x_A^{fluid} and x_B^{fluid} as functions of e^{-A} and e^{-B}, which again is functions of the material properties of the lipids A and B, namely $\Delta H_{i,0}$ and $T_{m,i}$, aswell as temperature as a variable. Finally, using the fact that the total membrane consists of a fluid part x^{fluid} and a gel part x^{gel} and that the sum of these to fractions must equal 1, one obtains

$$x^{fluid} = \frac{x_B^{gel} - x_B}{x_B^{gel} - x_B^{fluid}} \quad \text{and} \quad x^{gel} = 1 - x^{fluid} \tag{2.9}$$

Which is known as the lever rule. This allows you to calculate the fractions of gel and fluid phases as a function of temperature. This can now be used to calculate phase diagrams like the one below
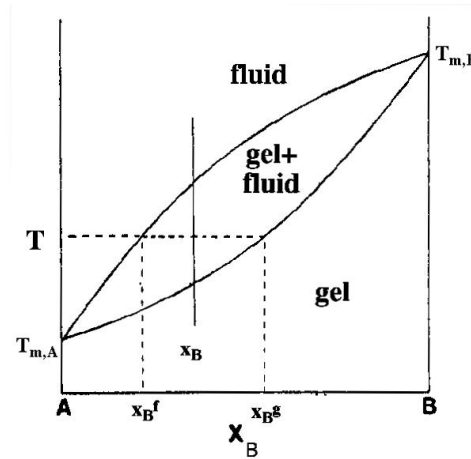

Figure 2.2: Example of a phase diagram, [4].

In the phase diagram of the ideal solution there are three regions describing different phases: A gel phase, a phase of coexistence between gel and fluid and finally a fluid phase. On the x-axis, one sees the fraction of lipid B and therefore one can deduce the fraction of lipid A from this axis too. On the y-axis the temperature is shown, ranging from slightly under the phase where gel and fluid coexists to a little above this phase, since this is the temperature region of interest. When one considers a mixture in the gel phase, temperature and lipid composition can be varied freely and the mixture will still be in the gel phase. This is true as long as one does not cross the border line to the coexistence region. The same is true for the all fluid phase. Temperature and concentration variations can be made as long as the border line to the coexistence region is not crossed and will not result in a phase change. In the coexistence region this is not the case. At a given temperature T and a lipid concentration x_B the amount of lipids in the gel phase, x_B^{gel}, and fluid phase, x_B^{fluid} are determined by the lever rule. This also means, that upon varying temperature, one will change the lipid concentrations in accordance to the lever rule, and the other way around if one varies the lipid concentration.

2.3 Nerve signal transmission

Since neurons play an important role in this project, and their sole purpose is to transmit signals, the way signals are transmitted deserves a certain interest. At present there are at least two different ways of looking at the nerve signal, namely the Hodgkin-Huxley model from 1952, [3], which is the well established and prevailing theory in the neurology. On the other hand there is the newer theory of solitons, a thermodynamic model og signal transmission which attacks some of the flaws that still are present in the Hodgkin-Huxley model. In the subsequent section a short introduction to these two models will be given.

Hudgkin-Huxley model

When one talks about a travelling neural signal in respect to the Hodgkin-Huxley model, one is taking about an action potential. This is a voltage pulse travelling down the neuron. This pulse is induced by a movement of ions across the nerve cell membrane. Most important are the ions Na^+, K^+ and Cl^-. A difference in concentration of these ions between the interior and exterior of the nerve is maintained by a concentration gradient and a electric field induced by the charges of these ions. The result is a potential difference between the two sides of the nerve membrane. By introducing the concept *equivalent circuit* the nerve is described as a circuit where current (caused by the moving ions) can flow through voltage gated channels.
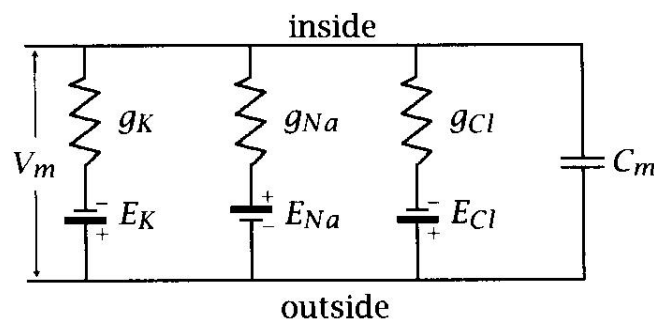

Figure 2.3: Equivalent circuit, [5]

E_{ion} is the potential induced by the given ion and g_{ion} is the conductance (inverse of resistance) of the ion through its channel. C_m is the capacitance of the membrane. The sum of the different potentials is the total potential difference (called the resting potential) between the two sides of the nerve. Nerve signals are then triggered by an external depolarization of the membrane. This depolarization allows Na^+ to flow through its respective channel, and this sodium ion current then causes a further depolarization, allowing nearby sodium channels to open for Na^+ passage across the membrane aswell and an action potential will now propagate down the nerve. This is a very simplified description of the model, but it should be able to describe the essence of the Hodgkin-Huxley model, namely voltage controlled movement of ions through ion specific channels, which causes a moving action potential. Differences in ion concentrations and action potentials have been computed and measured, and the Hodgkin-Huxley model has shown great agreement with experimental results.

Soliton model

The most important issue with the Hodgkin-Huxley model is the fact that no heat is dissipated during an action potential, this is an experimental fact, [5]. This does not fit into a theory where current flows through a resistor (flow of ions through an ion channel), where heat should dissipate due to friction. Therefore the soliton model was made. Solitons are travelling pulses that do not change shape or lose energy, much like a sound wave. When a sound wave propagates it causes a local change in pressure, and thereby a change in density of the medium. The nerve membrane, where most lipids are in the gel phase, is so close to its phase transition that in an action potential the phase will change, causing a change of density. This means that the action potential can be seen as a travelling change of density, a density pulse.

3 Methods

As stated in the introduction most of this project is based on the use of an AFM. Therefore this section will be about the principles behind the AFM, sample preparation and the execution of the experiments.

3.1 Experimental method

This will be an introduction to the mechanics of the AFM. First of all we want to know what an AFM actually is. An AFM belongs to a class of microscopes abbreviated SPM, which is short for scanning probe microscopy. As the name says, this type of microscope uses a probe moving across whatever sample, one wants to examine, instead of ordinary microscopes that use magnifying lenses. The main part of this scanning probe is the AFM cantilever. The cantilever sits at the end of a small chip, and it is possible to have several cantilevers at the same chip. The upper surface of the cantilever is coated with a reflective material like aluminium or gold. On the front is the cantilever tip which is the part of the AFM that faces the sample surface.
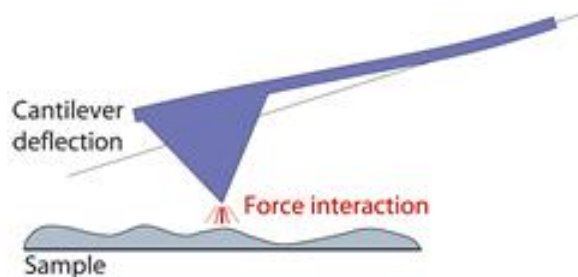

Figure 3.1: AFM cantilever and a sample, [14].

Although the schematic drawing above nicely displays the setup of cantilever and sample, it gives the wrong impression of the dimensions that are present. The tip is much smaller than the rest of the cantilever. When the cantilever tip is moved across a sample surface the rest of the cantilever is deflected in accordance to Hooke's law by the forces acting between the tip and the sample. By targeting a laser on the upper surface of the cantilever and letting this be reflected onto a photodetector (Quadrant photodiode), one can measure the deflection of the cantilever.
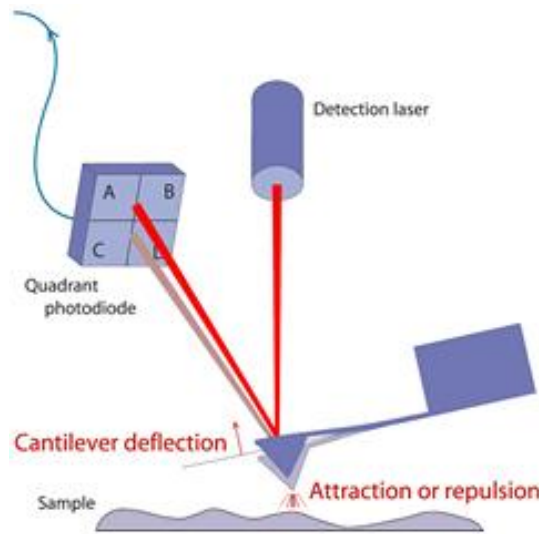
Figure 3.2: Whole AFM cantilever setup, [14].

Fig. 3.2 gives a good feeling of how an AFM works. As the cantilever has approached the surface of the sample, one can allign the laser beam reflection so that it will hit the center of the photodetector to detect deflections of the cantilever as it traces the sample.

3.2   AFM operating modes

Although the only operating mode used in this project is the contact mode, both this and the other most common operation mode, intermittent contact mode, deserves to be mentioned, since both ways of using the AFM are important. In the essence of the project contact mode will be mentioned first. As the name says, this way of scanning a surface includes direct contact between the tip and the sample. The principle is that one wants to keep the force between sample and tip constant. This is done by choosing a given setpoint value (a parameter given in volt, which is proportional to the deflection, which in turn is proportional to the force between sample and cantilever). When an appropiate value is chosen, usually less than 1 volt for biological samples, this will be the constant deflection during a measurement. This constancy is obtained by a feedback loop between the laser-photodetector and the AFM electronics. The way that the AFM produces pictures is then by moving the entire cantilever up and down, always keeping the deflection constant, visualizing this movement by a topographic picture of the sample.
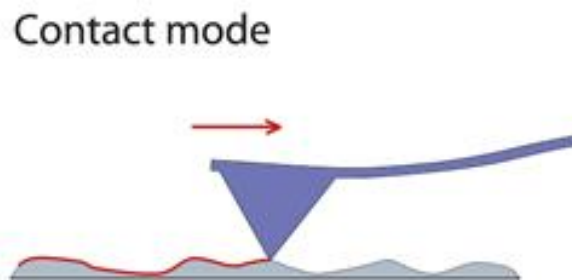

Figure 3.3: AFM in contact mode, [14].

The movement of the cantilever is done by a small piezoelectric motor. Piezoelectricity is the ability of certain materials to generate an electric field when a given stress is applied to them. The reverse effect is used in the AFM. By applying an electric field the piezoelectric crystal that the motor consists of can change its width and thereby move the cantilever up and down.
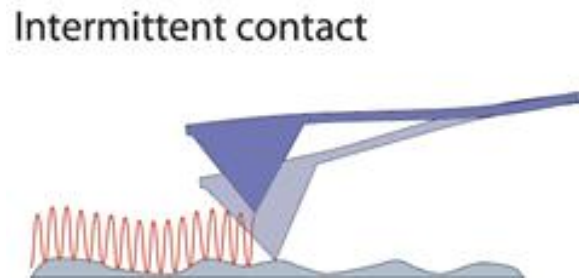
Intermittent contact

Figure 3.4: AFM in intermittent contact mode, [14].

The other of the two most common operating modes is the intermittent contact mode. In this mode the cantilever is oscillating at or near its resonance frequency. It is also the piezo-electric crystal that is responsible for this movement. In this mode the tip of the cantilever will also be in contact with the surface of the sample, but it will only be for a brief period of time before it is lifted away vertically from the surface during the oscillation. By tapping the surface of the sample the oscillation amplitude is reduced, and it is this change that is measurable. Like in contact mode, a certain setpoint is chosen (in intermittent contact mode this is inversely proportional to the force between the sample and tip) which will determine the amplitude of the oscillation when tapping the sample. When the tip moves over an obstacle in the sample a feedback loop with the laser, photodetector and AFM electronics will make sure the amplitude stays constant. It is these adjustments that are measurable and give rise to the produced images.

The reason for choosing between the two modes of operation is their applications. First of all the contact mode is straight forward to use, because in intermittent contact mode complications happens more often on soft samples, [12]. Other arguments for choosing contact mode is that it is better suited for faster scans and scans of steep edges. The advantage of intermittent contact mode is that it to a lesser degree than contact mode will drag loose objects across the surface when scanning and allows one to obtain phase images which gives information about surface proporties like elasticity. Further more the amplitude in intermittent contact mode is less sensitive to variations in temperature and liquid conditions than deflection is in contact mode.

Earlier it was mentioned that only contact mode is used in this project. The reason was basicly that this mode was easy to understand and use, although it might not produce as good pictures as intermittent contact mode does. Nevertheless by looking at pictures made by both modes, on the same types of samples that I used, it was decided that contact mode would be sufficient, [1].

3.3 Sample preparation

During the project three different kinds of samples have been imaged. These three are respectively DPPC, a mixture of DMPC and DLPC and finally the nerve bundle of a crayfish tail. Here the preparation of these samples will be presented:

DPPC: We want a 10 mM DPPC solution. This does not have to be very precise since the only purpose is to make images and not calculations. The reason for choosing this concentration is that it is suitable to produce regions without any lipid bilayers, aswell as regions with lipid bilayers where one or more layers are on top of each other, when put on mica[1]. DPPC has a molecular weight of 734 g/mol, so by taking around 15 mg and dissolve this in 2 mL of millipore water we get the right concentration. At this point the lipids will form giant vesicles, which are multilamellar vesicles that will not bind to the mica and form the bilayers that we are looking for. Therefore the suspension, which is milky white at this point, will be sonified. A sonifier is a device that generates ultrasound, which can be used in liquid suspensions to disrupt for example multilamellar vesicles so they instead will form small unilamellar vesicles. The sonification lasted for 20 minutes until the suspension changed from milky white to a transparent. The suspension was kept above phase transition (41°C, [13]), to prevent the small vesicles to fuse back into multilamellar vesicles. One droplet of the suspension was then put on cleaved mica placed in a small petri dish. Letting the suspension incubate on the mica for 30 minutes was found sufficient to watch regions with bilayers, but later experiments with longer incubation time like one to two hours gave better results. After incubation excess vesicles was gently washed with millipore water. After removing the water again with a pipette, clean millipore water was put into the petri dish so that the sample was covered in water.

1:10 DLPC/DMPC mixture: This sample preparation is slightly different from the one mentioned above. The reason is that for the two lipids to mix, they independtly have to be dissolved in an organic solvent. Therefore 2 mL 5 mM DMPC and 200 μL 5mM DLPC, both dissolved in a mixture of dichloromethane and methanol[2], was mixed. Afterwards the mixture was heated in a bath of water with a controlled temperature until the organic solvent was evaporated and only the mixed lipids were left. The dry lipid mixture was placed in a vacuum chamber for fifteen minutes. This ensures that whatever is left of the organic solvent will evaporate under the low pressure. 2.2 mL of water was then added to obtain a 5 mM 1:10 DLPC : DMPC mixture. At this point the rest of the procedure is the same as for the single lipid solution. First the solution is sonified, then put on a piece of cleaved mica etc.

Crayfish nerve: First a piece of cleaved mica is placed in a small petri dish. The mica is then fixed to the bottom of the dish with a fast drying silicone like compound. Meanwhile the nerve of the crayfish was cut out by Rolf J. Pedersen, member of the Membrane Biophysics Group. The nerve that has been used is called nerve 3, which basicly just refers to its position in the crayfish. It is a motor nerve, which means that it only can send signals one way, that is away from the central nerve that goes down the crayfish tail, and towards the muscles that it is connected to. It is normally 6 mm long $\pm$ 2 mm. This is actually not a single nerve but a bundle of nerves held together by tissue, much like a myelin layer. A cross section of a bundle like this can be seen below where neurons are marked with a *.

---

[1]Mica is a mineral that can be cut into very flat pieces, and therefore it serves very well as a substrate for AFM imaging.

[2]The mixture is 2:1 dichloromethane : methanol by volume. Dichloromethane is good for dissolving apolar lipids whereas methanol is good for dissolving polar lipids.

Figure 3.5: Cross section of a nerve bundle like the one used in the experiment

It was possible to place the nerve bundle on the mica while most of the muscle fibres etc. attatched to the two ends of the nerve was put on each side of the mica. This ensured that the nerve bundle was stretched out and stayed relatively fixed. The muscle fibres were then fixed to the bottom of the petri dish with more of the silicone compound. The petri dish was then filled with a buffer resembling the natural environment that the crayfish was living in. This was also prepared by Rolf J. Pedersen.

3.4 Execution of the experiments

The first thing to be done is to choose a type of cantilever. There are many kinds of cantilevers with different properties, but only one kind has been used throughout this project and therefore this has been of minor interest[3]. When a proper cantilever has been choosen and attached to the AFM, one can begin to prepare AFM imaging as soon as the sample one wants to examine has been placed underneath the cantilever. For samples in liquids it is important that there is enough liquid to cover the cantilever and preferably a little more. Surface tension can disturb the experiment.

First thing to do is to indentify the cantilevers in an optical microscope on which the AFM is mounted. Once identified, one can switch view to look at the cantilever through the camera of the AFM instead. This allows one to see the laser beam, which has been filtered out in the optical microscope to avoid eye damage. Now allign the laser so that it hits the reflective surface of the cantilever. Though the laser beam is hitting the cantilever, one can not make measurements at this point. The laser has to be reflected by a small mirror[4], so this reflection will hit the photodetector. One can first adjust the mirror and then the position of the photodetector. The principle is that the software used along with the AFM shows a window where one sees a small red dot and four blue squares representing the photodetector. The laser beam (red dot)has to be in the center of the four squares to optimize detector sensitivity to changes in the laser position. First one has to adjust the mirror. Adjusting the laser and mirror is part of the course grained allignment, which should not be needed more than once if one wants to examine samples in the same environments e.g. same types of liquids. Fine grain allignment is the adjusting of the photodetector and lets one move the red spot exactly to the center of the four squares, ensuring good imaging. This adjustment might be needed

---

[3]Cantilevers can vary in spring constants, reflective covering of the backside, resonance frequency, shaping of the cantilever tip and shape of the cantilever in general.

[4]This mirror is for course grain adjustment, for instance to correct for refraction by water when imaging in this medium.

regularly because of cantilever drifts as a result of changing temperatures and possibility of slow adaption to these changes by the cantilever. At this point one has to choose operating mode. As stated several times, only contact mode has been used in this project, and therefore the following procedures is in respect to this choice. Differences might occur when making intermittent contact measurements.

Now one can approach the sample with the cantilever. Three parameters was found sufficient to change, to make successful approaching, namely Set point, approach IGain and z-range. Set point has already been mentioned elsewhere. The approach IGain is a parameter used by the AFM when adjusting the height to keep the cantilever deflection constant. There is also a separate IGain value for the approached cantilever, used when imaging. Z-range is the height range limit in which the piezoelectric motor can move and can be varied from values between 15 μm and 1.5 μm, the lower the range the better the resolution. Insuccessful approaches is recognized mainly by a fast drift of the piezoelectric motor either to being fully extended or retracted. Extention might be caused by the sample being pushed down by the cantilever, due to the lack of a sufficiently hard substrate that the sample is placed on or possibly deformation of the sample. Retraction might be caused by a tip that is too sharp, which causes the tip to sink into the sample. Another possibility for unsuccessful approach is a high pitched sound comming from the apparatus when approaching. This is caused by oscillations in the vertical deflection, [12]. One can let the approaching continue for a short time after the sound has started, since it usually starts near the sample surface and might stop when reaching the surface. Otherwise the approaching should be aborted and and one can try again with new parameters. When a successful approach has been made, one simply starts running a scan and the AFM will start imaging whatever region of the sample one has choosen by moving the cantilever tip along a straight line across the sample, then move a small step sideways and start scanning the next line etc. The execution of the experiments can basicly be written in the following points:

- Mount cantilever and sample

- Indentify cantilever in optic microscope

- Course grain allignment: Adjust laser to hit the cantilever and adjust mirror (if necessary) to reflect the laser beam onto the photodetector

- Fine grain allignment: Adjust photodetector

- Approach sample

- Run scan

4 Results and Discussion

The images made will be presented and discussed in the following section. All data have been analysed with the program Gwyddion which allows one to level data, substract background, remove artifacts etc. The AFM produces raw data of the height of the sample investigated at a given coordinate from the movements of the piezoelectric motor, and it is this data that one is able to convert into analysable images. This means that the images shown below are not exact images of how the surface looks like, but the 'feeling' of the cantilever on the sample surface. It is a color gradient that shows the difference in height and the lowest lying parts of the sample will be represented by black/dark brown colors whereas higher lying regions will be shown in light brown/white. Another feature of Gwyddion is that it allows one to draw height profiles across the sample and see the height differences between different parts of the sample.

4.1 DPPC

The first sample to be analysed was the DPPC sample. It is the most simple of the three samples since it only consists of a single lipid put on a piece of mica. The experiment was performed at room temperature and since DPPC has a melting temperature at $41°C$ all lipids should be in the gel state. The best of the images produced can be seen below.
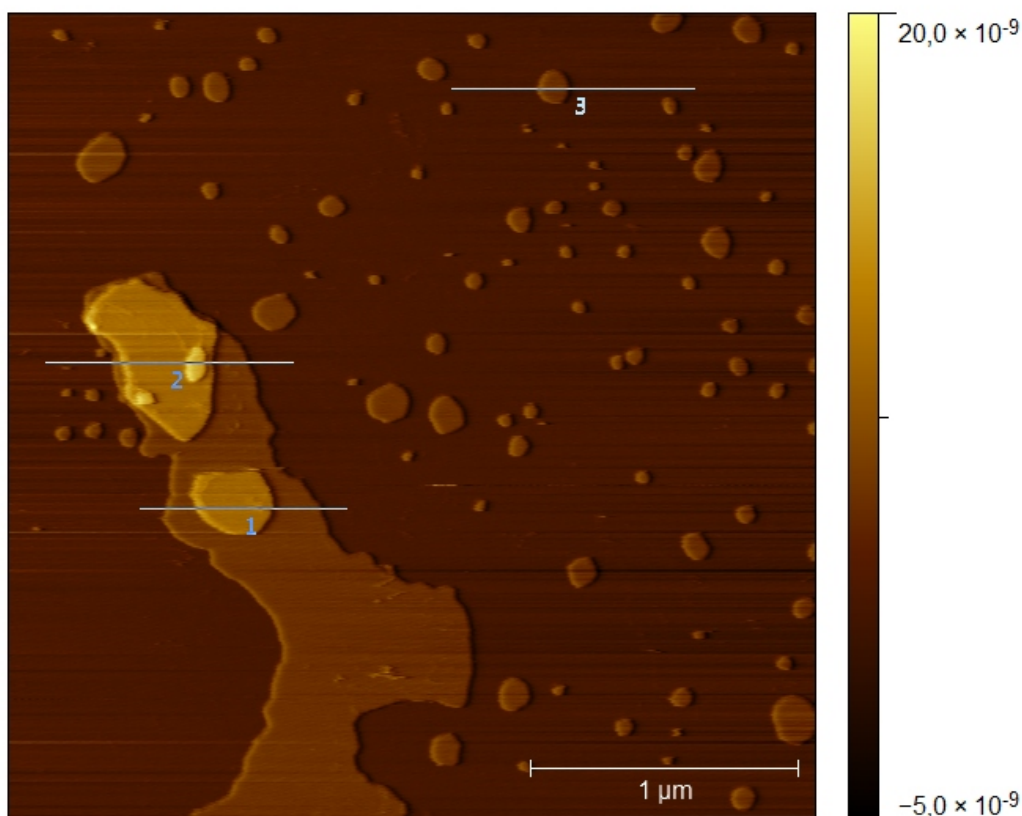

Figure 4.1: DPPC on mica surface.

The dark brown region covering most of the image[1] is the supporting mica surface and is fixed to be at a height of ~ 0 nm. Several small 'islands' can be seen in a lighter brown and these regions are the lipid bilayers fixed to the mica surface, the same color of these regions indicates that they all have the same height. At the large region of lipid bilayer smaller regions can be seen on top of this. These are also lipid bilayers located on top of the first one. The black lines does not have any physical interpretation related to the sample and are most reasonably caused by external disturbances like people walking next to the AFM etc.[2] The lines with the numbers 1 through 3 represent height profiles of the sample, which looks like this.

---

[1]Longer incubation time would most certainly have led to a more covered mica surface.

[2]Scan speeds are usually between 1 to 2 seconds per line, a reasonable time it would take a person to walk by the apparatus.
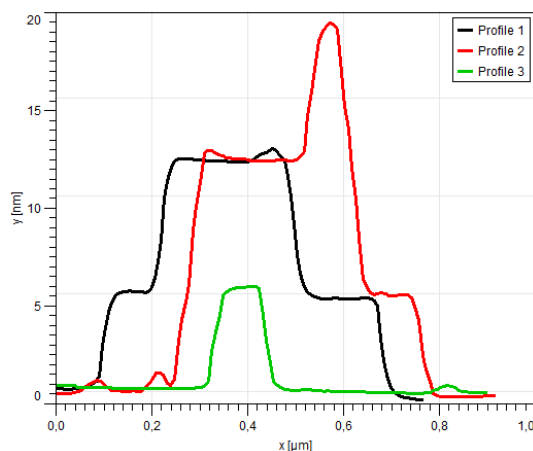
Figure 4.2: Height profile of DPPC.

The first thing one notices is the height of both profile 3 and the lower parts of profile 1 and 2 all have the same height, which is a little less than 5 nm. From the litterature, [6], it is given that the thickness of a lipid bilayer is approximately 4.7 nm. At this point the experiments are in good agreement with other experiments which indicates that things have been done right. On the other hand when, one looks at the lipid bilayers lying upon the first one (profile 1 and 2), one sees that these lipid bilayers have a height of approximately 7 nm each. The reason to this difference of approximately 2 nm between a single lipid bilayer and several lipid bilayers on top of each other is that when two layers are on top of each other there will be a layer of water in between, causing the extra height of 2 nm, [1].

4.2   1:10 DLPC : DMPC

The second sample is the mixture between DLPC and DMPC. The reason for making this mixture was to get an image of lipids in the melting transition. In the phase diagram this means the coexistence phase where gel and fluid lipids are both present. This image of the melting transition is possible because 1:10 DLPC : DMPC has a melting temperature about 22 °C, which corresponds to the room temperature. The melting temperature can be seen from the heat capacity profile.
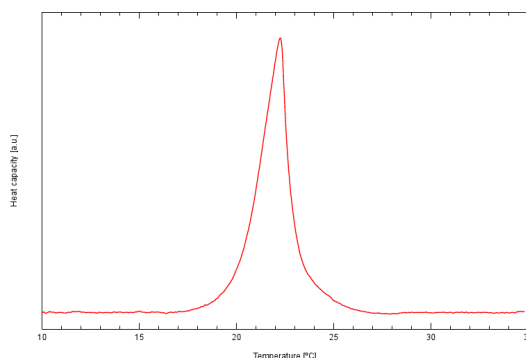

Figure 4.3: Heat capacity profile of 1:10 DLPC : DMPC

This profile was made by Andreas Blicher from the Membrane Biophysics Group with a 1:10 DLPC : DMPC mixture in a 150 mM KCl solution. The mixture was sonified just like the mixture in the experiments made in this project. The y-axis is in arbitary units, but that is not important at this point, since we are only interested in the melting temperature and the shape of the curve. One can see that the profile is relatively narrow and that even though it represents two lipids, only one peak can be seen. This is a good indication of ideal solution behavior, which is what one would expect to see now. From the first experiments with the mixture the following image was obtained.
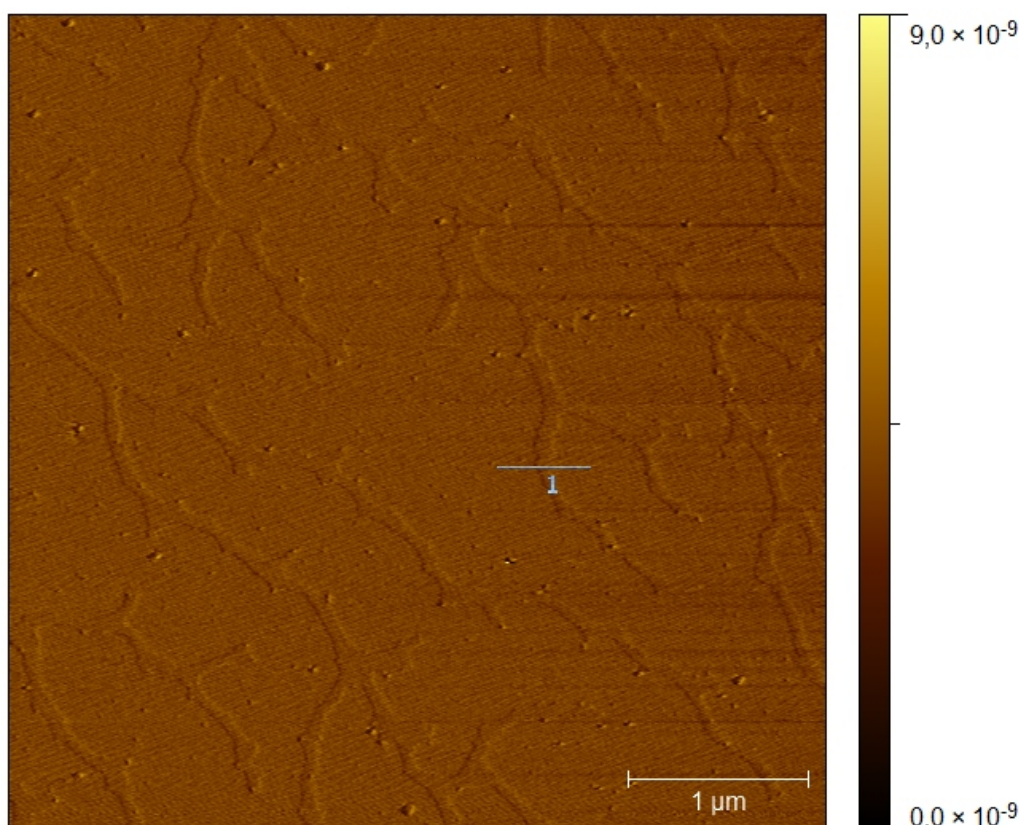

Figure 4.4: DLPC:DMPC above melting temperature, supported on mica.

Due to longer incubation time of these samples, one does not see any regions of mica, and therefore one should not look at the color scale to the right and expect the bilayer to be 9 nm high. One sees a general change in structure in respect to the previous image and notices thin 'river-like' regions slightly lower than the rest of the image. For further investigation a height profile has been made across one of these 'rivers'.
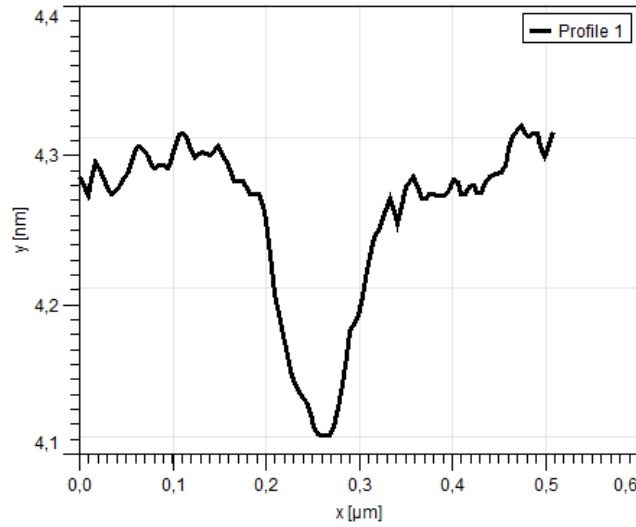
Figure 4.5: Height profile of DLPC : DMPC above melting temperature

The important thing to notice in this image is the smaller height difference of only ~ 0.2 nm. Fluctuations are bigger in this image, but it seems reasonable since we now got a mixture of different lipids close to the melting temperature. DLPC and DMPC have respectively 12 and 14 carbons in their hydrocarbon chains whereas DPPC has 16. Therefore the thickness of DLPC and DMPC bilayers are accordingly smaller. All three lipids have the same headgroup, and when looking at Figure 2.1 the headgroup seems to occupy something like 40 percent of the total length. An estimate of the lipid bilayer thickness would be that DLPC chain lenght is 12/16 of DPPC chain lenght and that the headgroup thickness stays the same. The ratio between DMPC and DPPC chain lenght would be 14/16. From the litterature one has that the thickness of DPPC in the fluid phase is in the order of 3.9 nm[3]. If one further estimates that the main reason to the change in thickness between gel and fluid state is the disordering of the hydrocarbon chains, one can expect that the headgroup thickness is approximately the same in the two states. This means that the headgroup thickness is approximately 1.9 nm, when estimated to be 40 percent of the DPPC thickness. One can now construct a table of the estimated differences in bilayer thickness.

Lipid and number of carbonatoms in the respective chain	Gel chain length (nm)	Fluid chain length (nm)	Difference in chain lengtht between phases (nm)
DPPC - 16	4.7 - 1.9 = 2.8	3.9 - 1.9 = 2.0	0.8
DMPC - 14	(14/16)·2.8 = 2.5	(14/16)·2.8 = 1.8	0.7
DLPC - 14	(12/16)·2.8 = 2.1	(12/16)·2.8 = 1.5	0.6

Table 4.1: Table of estimated chain lengths.

One sees from this table that the expected height difference should be approximately 0.7 nm since the mixture mainly consists of DMPC. This is not consistent witht the experimental result of 0.2 nm. A reasonable explanation would be that both lipids were in the fluid

---

[3]Mean of the three different values presented in [6].

state. Assuming this along with the estimate of the lipid bilayer thickness, one would expect a height difference between DLPC and DMPC, both in the fluid state, of 0.3 nm. The numbers in the table are rounded so it certainly seems possible that the image is showing both lipids in the fluid state. Measuring the temperature of the laboratory indeed showed that the temperature was about 25°C which is above the melting temperature. By lowering the room temperature to 22°C the following image was obtained.
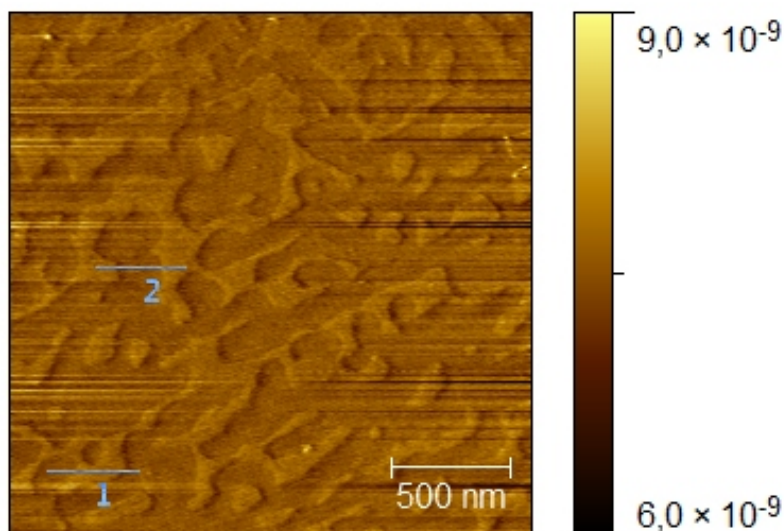

Figure 4.6: DLPC : DMPC at melting temperature, supported on mica.

First of all, one notices that the structure is different from the image obtained earlier when imaging this mixture. But when looking at the height profile one sees that the difference indeed is around 0.9 nm, which fits better into the expected difference of about 0.7 nm.
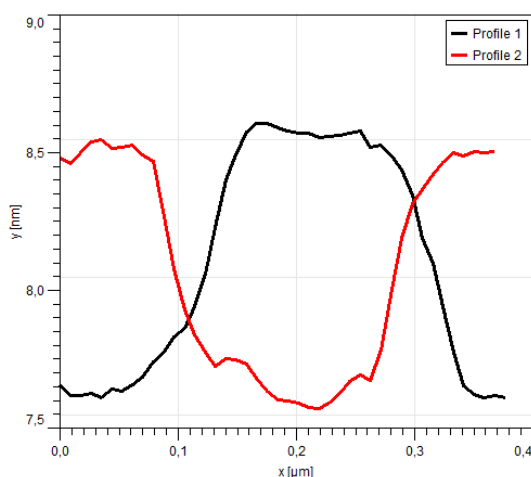

Figure 4.7: Height profile of DLPC : DMPC at melting temperature.

This means the the lower lying regions are the lipid mixture in the fluid state and the higher lying regions are in the gel state. The fact that one recognizes DLPC and DMPC as different regions in Figure 4.4 indicates that 1:10 DLPC : DMPC is not an ideal mixture, since one in this case would expect a single fluid phase, as one would have guessed from the heat capacity profile. However this immiscibility may be caused by the binding of the lipid films to the mica surface, so that the mixture indeed shows ideal solution behavior when forming vesicles, as is the case when the heat capacity profile is measured.

4.3 Crayfish nerve

The last sample was the one of a crayfish nerve bundle. The difference between this experiment and the other two is that it is not known exactly what to expect, compared to for example a bilayer thickness of 4.7 nm. The first images of the nerve was made without fixing it to the mica surface, but only to the bottom of the petri dish. This resulted in images that basicly was just lines without any recognizable structures. By fixing the nerves the images became slightly better. The images are still blurry and dominated by lines caused by the lateral drag of the cantilever on the nerve. This effect could be seen on the camera attached to the AFM, and it was clear that though minimizing the dragging, the fixing did not stop it totally. Two of the images produced when the nerve bundle was fixed to the mica substrate can be seen below.
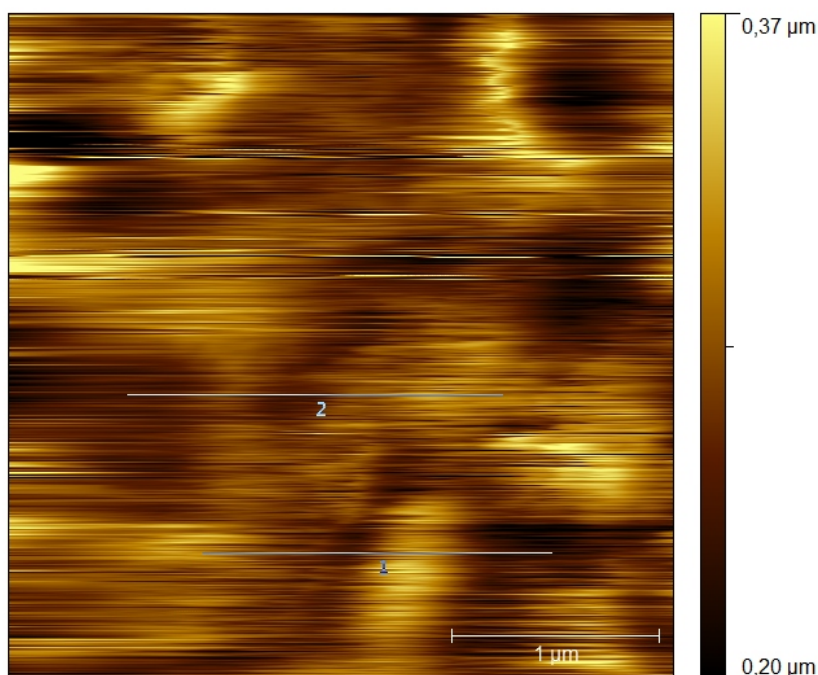

Figure 4.8: First image of crayfish nerve bundle.

This is the first picture of the crayfish nerve bundke. As stated above it is difficult to deduce anything general from this picture. A second image of the nerve bundle has been made and looks like this.
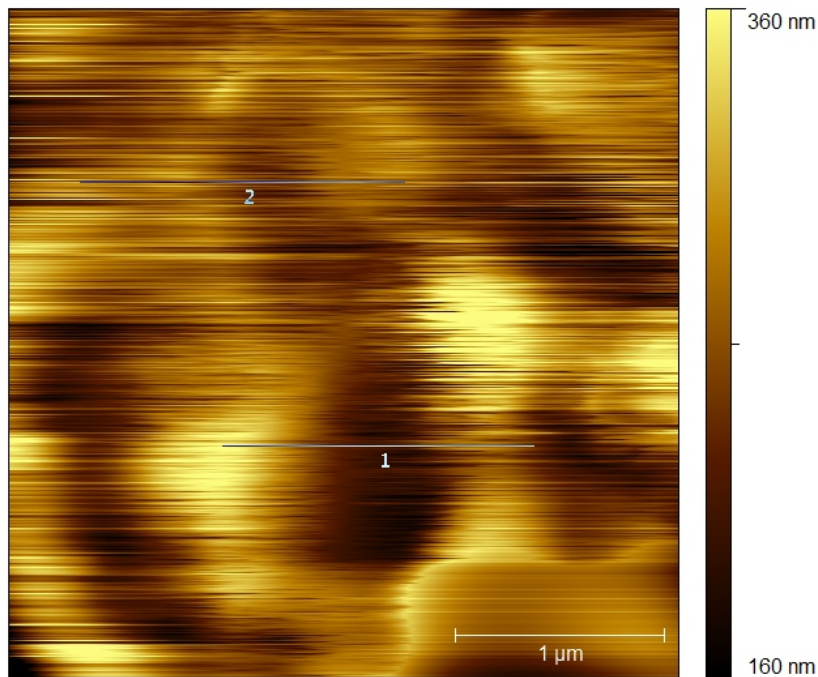
Figure 4.9: Second image of crayfish nerve bundle.

Height profiles from the two images have been made to compare the structures in the images. Although not saying much about nerve bundle, one at least would expect structures of the same orders of height to ensure that it really is the crayfish nerve that is being imaged. These profiles look like this
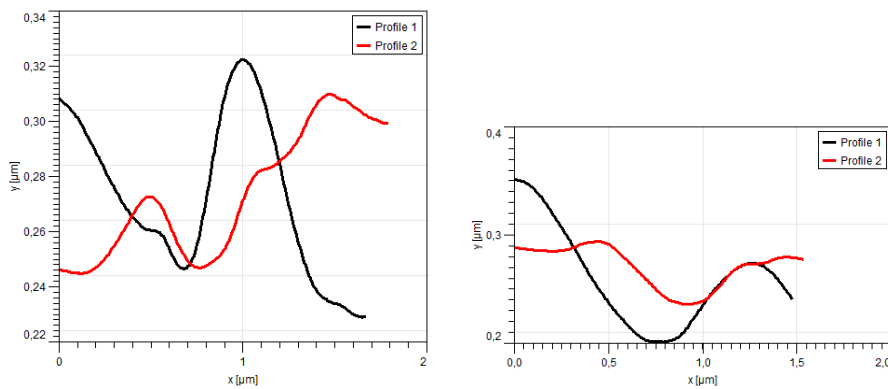

Figure 4.10: Crayfish nerve bundle height profiles. Left profile is from the first image, right is from the second.

One sees that the structure height indeed is in the same order of magnitude, which could indicate that it is the crayfish nerve bundle that is being imaged.

5 Conclusion

Generally the project can be split into two parts. The first part with the experiments involving DPPC and DLPC : DMPC and the second part with the crayfish nerve bundle. Through the first part of the project it was known how the images should look like, e.g. bilayer thickness and phase behavior, and it was actually possible to produce images that looked like one expected. The main reason for doing this part of the project was to get used to work with the AFM of soft samples. This was indeed successful since nice images were produced, and as an extra result the image of the mixture above its phase transition were produced, and a possible explanation to this behavior was given.

The second part of the project was more tricky. First of all there is the quality of the images. Time was spend in the laboratory to indentify problems resulting in the lines and blurry images. Some of the same behavior had been seen when working with the lipid films, but at that time it was problems with the cantilevers, and since choosing another cantiliver for the nerve did not help, it most certainly was something else that caused the problems. At that time the nerve was fixed, first to the bottom of the petri dish, which improved images slightly, and then to a piece of mica for even more improvement. Still the images are very blurry, and since the nerve bundle could not be totally fixed with the setup used in this experiment, it can be the explanation of how to produce good quality images, simply by better fixing of the nerve bundle. Another solution might be to use intermittent contact mode, which as stated earlier, causes less lateral drag on the samples. This way disturbances of the nerve bundle might be avoided aswell.

Finally one could look at the perspectives of this AFM imaging of nerves. One could argue that although producing pretty pictures of a section of crayfish nerve bundle is fun, it might seem rather useless. However it is well known that during the action potential of a nerve signal, the nerve changes thickness and length, [16], [17] and [18]. These are properties measurable by the AFM. Though it have never been the purpose of this project to distinguish whether the Hodgkin-Huxley model of the soliton model (or maybe something else) is the right way of looking at propagating nerve signals, experiments with nerve bundles (and eventually single nerves)and an AFM might help to shed light on this discussion.

Bibliography

[1] Vitaliy Oliynyk, *Experimental study of lipid membranes: lipid domain formation and peptide aggregation*, Ph.D. thesis, Niels Bohr Inst. Copenhagen, Univ. Göttingen, 2005

[2] S. J. Singer & G. L. Nicolson, *The fluid mosaic model*, Science 175: 720-731,

[3] A. L. Hodgkin and A. F. Huxley, *A quantitative description of membrane current and its application to conduction and excitation in nerve - Part I p. 500-504*, J. Physiol. 117 p. 500-544, 1952

[4] T. Heimburg, *BIOPHYSICS OF MEMBRANES - BIOPHYSICS II*, course material 2010

[5] T. Heimburg, *BIOPHYSICS OF NERVES - Biophysics IV*, course material 2010

[6] T. Heimburg, *Mechanical aspects of membrane thermodynamics. Estimation of the mechanical properties of lipid membranes close to the chain melting transition from calorimetry*, Biochimica et Biophysica Acta 1415 147-162, 1998

[7] T. Heimburg and A. D. Jackson, *On soliton propagation in biomembranes and nerves*, Proc. Natl. Acad. Sci. USA. 102: 9790-9795, 2005

[8] Gordon L. Fain, *Molecular and Cellular Physiology of Neurons - Chapter 1-5 p. 1-170*, Harward University Press, 1st edition, 1999

[9] Jeremy M. Berg, John L. Tymoczko and Lubert Stryer, *Biochemistry - Chapter 12 p. 326 - 350*, W. H. Freeman and Company, 6th edition, 2006

[10] G. Binnig, C. F. Quate and Ch. Gerber, *Atomic force microscope*, Physical Review Letters, volume 56 number 9, p. 930–933, March 1986.

[11] *JPK Nanowizard® II User manual SPM software release 3.3*, 2009

[12] *Nanowizard® AFM Handbook version 2.2*, 2009

[13] www.avantilipids.com

[14] www.jpk.com

[15] www.sonifier.com

[16] K. Iwasa, I. Tasaki and R.C. Gibbons, *Swelling of nervefibers associated with action potentials*, science 210 p. 338-339, 198

[17] K. Iwasa and I. Tasaki, *Mechanical changes in squid giant axons associated with production of action potentials*, Biochem. and Biophys. Res. comm. 95 p. 1328-1331, 1980

[18] I. Tasaki, K. Kusano and P.M. Byrne, *Rapid mechanical and thermal changes in the garfish olfactory nerve associated with a propagated impulse*, Biophys. Journal 55 p. 1033-1040, 1989